

Effect of Partial Spatial Coherence on Image Sharpness

Silin NA

Kanghae Precision System, Hwasung 18487, Korea

Doocheol KIM · Younghun YU*

Department of Physics and Research Institute for Basic Sciences, Jeju National University, Jeju 63243, Korea

(Received 02 September 2019 : revised 04 November 2019 : accepted 04 November 2019)

Holographic displays are coherent light processing systems based on interference and diffraction, thus they generally use coherent light source. Highly coherent light makes some undesired effects, such as speckle noise. We studied how the degree of spatial coherence affected the image sharpness of a holographic display. We used rotating ground glass to control the degree of spatial coherence and a non-interferometric holographic system for imaging with simultaneous determination of the spatially coherent illumination. Image sharpness is related to both the temporal and the spatial coherence of the light source; our results demonstrate a direct relationship between spatial coherence and image sharpness.

PACS numbers: 42.40.Kw, 42.40.Lx, 42.30.Wb

Keywords: Digital holographic microscopy, Partial coherence, Image quality

I. INTRODUCTION

Holography, invented by Dennis Gabor, is a technique for measuring three-dimensional (3D) objects and realizing holographic displays (HDs) [1–4]. A reference and an object beam are required, and an interference pattern is generated by combining the two beams. Previously, the interference patterns were recorded on film plates. However, charge-coupled device (CCD) and complementary metal oxide semiconductor (CMOS) technology are now widely used for image capture, and computers are used for hologram reconstruction. The digital recording and reconstruction of a numerical hologram is known as digital holography (DH) [5–9], which is now feasible due to advances in megapixel CCD sensors with high spatial resolution. DH exploits the coherence of the light source; coherent light is applied extensively in numerous imaging techniques. One application of DH is the digital holographic microscope (DHM), which measures the 3D shape of an object based on interference. HD has emerging applications in augmented reality and virtual reality.

The main drawbacks of coherent laser-based imaging are speckle noise and distortions caused by parasitic reflections in the optical setup and the sample chamber itself. The presence of speckle noise severely degrades the quality of reconstructed images, which remains as one of the fundamental challenges in digital and optical holography. Optical methods such as reducing the spatial coherence of light sources, and computational methods including digital image processing and computer-generated hologram (CGH) computation algorithms [10–12] have been implemented for speckle reduction. Use of light-emitting diodes (LEDs) makes it possible to reduce the undesirable interference effects and speckle noise in HDs to a certain extent, at the expense of reduced resolution. Illuminating the hologram surface with a low-coherence light source, such as an LED, results in smoother images in comparison to high-coherence laser sources.

In this paper, we present a non-interferometric technique and optical system for fast quantitative imaging of objects under partially coherent illumination. We investigate the effect of source spatial coherence on the sharpness of the reconstructed images.

*E-mail: yyhyoung@jejunu.ac.kr



II. THEORETICAL MODEL

Optical imaging with temporal and spatial partially coherent light is inherently complicated and requires consideration of the complex mutual coherence function. In the stationary quasi-monochromatic case, it can be written as a product of the temporal and spatial coherence functions $T(t)\mu(r_1, r_2)$. Temporal coherence ($T(t)$) measures the average correlation of the light signals at any pair of moments between a wave from a light source and itself, delayed by time t . For a light source with a Gaussian emission spectrum, the temporal coherence length is given by:

$$l_c = \sqrt{\frac{2 \ln 2}{\pi n}} \frac{\lambda^2}{\Delta \lambda} \quad (1)$$

where c is the speed of light, n is the refractive index of the medium, λ is the central wavelength and $\Delta \lambda$ is the full width half maximum (FWHM) of the emission peak in the wavelength spectrum. Spatial coherence describes the correlation between two points in space, and the likelihood that they will interfere with each other when averaged over time. One measure of spatial coherence is the complex coherence factor μ_{12} [13,14];

$$\mu_{12}(x_1, y_1, x_2, y_2 : z) \approx \frac{\iint_S I(x, y) \exp[i \frac{2\pi}{\lambda z} (\Delta x x + \Delta y y)] dx dy}{\iint_S I(x, y) dx dy} \quad (2)$$

where (x_1, y_1) and (x_2, y_2) are the coordinates for the two light source in space, S is the light source size and $I(x, y)$ is the intensity distribution of the light source. The complex coherence factor μ_{12} is also given by $|\mu_{12}| \sim \exp\left(-\frac{s^2}{l_{sc}^2}\right)$, where l_{sc} is spatial coherence length. The l_{sc} is given by $l_{sc} = \frac{r\lambda}{2s}$, where r is the distance between two light sources. We can see that the degree of spatial coherence depends on the size (s) of the light source and the spatial coherence length (l_{sc}) [15]. Figure 1 shows double-slit simulation results with different spatial coherence lengths, i.e., different degrees of spatial coherence. The gap and width of the double-slit are 5 mm and 0.5 mm, respectively.

Figure 1 (a), (b) and (c) show the results with spatial coherence lengths of 10, 5 and 1 mm, respectively. The visibility, $v = \frac{I_{\max} - I_{\min}}{I_{\max} + I_{\min}}$, decreases as the spatial coherence length decreases. Figure 1 shows that the visibility depends on the degree of spatial coherence.

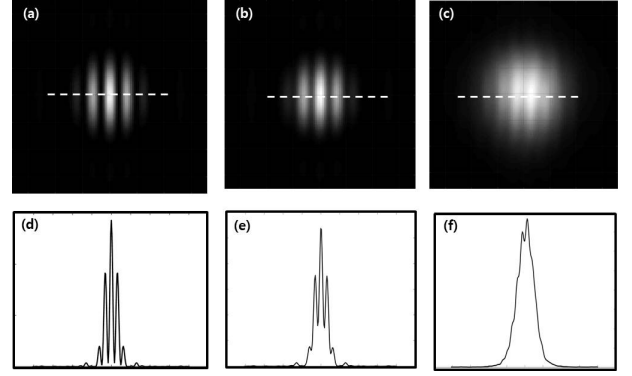


Fig. 1. Irradiance and profile of double-slit interference simulation results with different spatial coherence lengths. (a) (d) 10 mm; (b) (e) 5 mm; (c) (f) 1 mm.

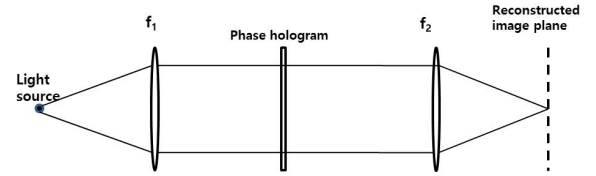


Fig. 2. A holographic display (HD) system with a phase hologram.

In a digital HD system, the sharpness of the reconstructed image depends on the degree of spatial coherence. To analyze their relationship, we consider an HD system, as shown in Fig. 2.

In the system, the waves from an ideal point source are collimated by a collimating lens and then illuminated on a phase hologram. After that, the diffracted beam is focused by a Fourier transform lens to its focal plane, on which we could see the reconstructed image (g_{out}). If we use the impulse response function of the system, the output is given as follows [13,14,16]:

$$g_{\text{out}}(x_2, y_2) = \iint g_{\text{in}}(x, y) h(x_2 - x, y_2 - y) dx dy \quad (3)$$

where $h(x_2 - x, y_2 - y)$ is the impulse response function of the display system and g_{in} is the light source or system input. The output image is the convolution of the input image with the impulse response function. The output can be expressed as Fourier transforms using the convolution theorem:

$$G_{\text{out}}(k_x, k_y) = G_{\text{in}}(k_x, k_y) H(k_x, k_y) \quad (4)$$

Where G_{out} , G_{in} and H are the Fourier transforms of g_{out} , g_{in} , and h , respectively, and k_x and k_y are the spatial frequencies. If the input image is a point source, G_{in}

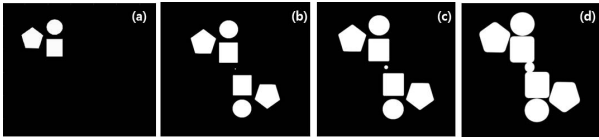


Fig. 3. Simulation results of the reconstructed image in HD system with different degrees of spatial coherence. (a) Object = 600×800 pixels; (b) (c) and (d) beam size = 1, 4, and 10 pixels, respectively.

will be the Fourier transform of a δ -function. This means that the reconstructed image retains all of the information in the spatial frequency domain if we use a point light source. However, if the light source has a certain size, some information in the spatial frequency domain is lost, which affects the output of the HD system. As discussed above, the extension of the light source is directly related to its spatial coherence, which will in turn affect the sharpness of the reconstructed image at the output by modifying its frequency information.

Figure 3 is the simulation result for a HD system with different beam sizes. Figure 3 (a) shows the object; (b), (c) and (d) are reconstructed images for beam sizes of 1, 4 and 10 pixels, respectively. The real image, virtual image and DC term can be seen. The DC term, which is located in the center, is the image of the light source. As discussed above, the sharpness of the reconstructed image decreases as the beam size increases, i.e., as the degree of spatial coherence decreases.

Figure 4 shows a schematic diagram of an HD system. One of the most common approaches to remove coherent noise is positioning a rotating ground glass (RGG) diffuser in the beam path, producing a partially coherent light source [17, 18]. We use two $1\times$ objectives for focusing the laser beam and collecting scattered light. We move the position of the ground glass to control the spatial coherence, and thus the beam size. The degree of spatial coherence is given by $|\mu_{12}| \sim \exp\left(-\frac{s^2}{l_{sc}^2}\right)$.

A 633-nm He-Ne laser was used as a light source. We used a CCD camera (Imperx) to record the holograms. The pixel size was $7.4\mu\text{m} \times 7.4\mu\text{m}$ and the pixel array was $1,024 \times 1,024$.

First, we measured the visibility according to different beam sizes with a double slit. The double slit was located at the “sample” position shown in Fig. 4. The gap and width of the double slit were 0.25 and 0.15 mm, respectively. The average intensity distribution of the

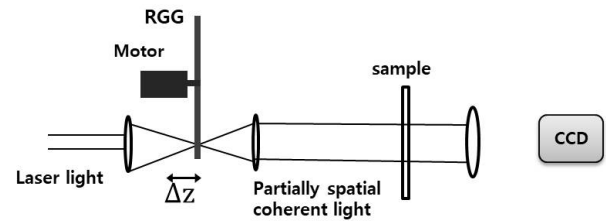


Fig. 4. Schematic of the experimental set-up. RGG, rotating ground glass.

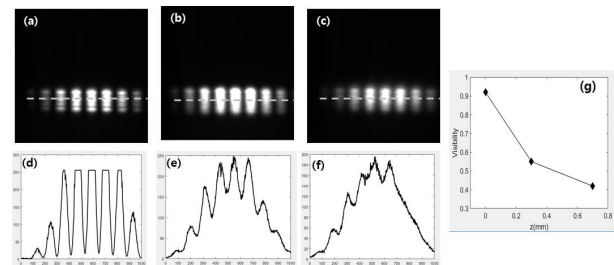


Fig. 5. Experimental results showing the interference pattern and profile for a double slit with different beam sizes. (a) (d) $\Delta z = 0$; (b) (e) $\Delta z = 0.3$ mm; (c) (f) $\Delta z = 0.7$ mm; (g) visibility with Δz .

interference pattern is shown in Fig. 5 according to different Δz , i.e., different beam sizes. Δz is the distance from the objective focal plane. The beam size on the ground glass increased as Δz increased.

Figure 5 (a), (b) and (c) are the intensity distributions of the interference patterns, and (d), (e) and (f) are profiles along the dotted line in (a), (b) and (c), respectively. Fig. 5 (g) is the visibility with Δz . We can see that the visibility of the interference pattern decreases as the beam size increases; this result was anticipated (see Fig. 1).

Next, we measured the sharpness of the reconstructed image in an HD system for different beam sizes. A phase-only hologram was located at the sample position in Fig. 4. The experimental results are shown in Fig. 6.

The holographic reconstruction of real and virtual images of the target can be seen in the figure; the zero order is located at the center. The image is of the emitting area of the light source; the sharpness of the reconstructed image increases as the size of the zero order decreases. Thus, the sharpness of the holographically reconstructed image increased with increasing spatial coherence.

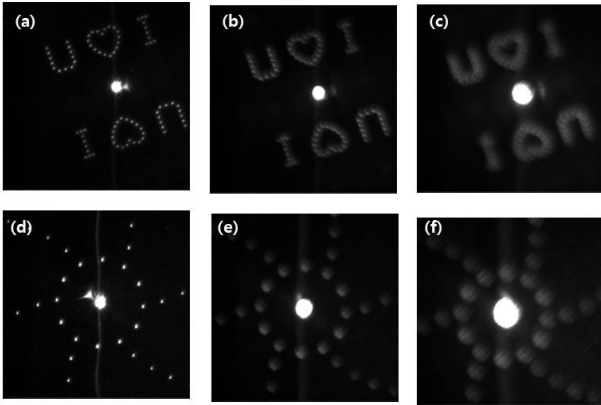


Fig. 6. Reconstructed holographic images in an HD system with different beam sizes. (a) (d) $\Delta z = 0$; (b) (e) $\Delta z = 0.3$ mm; (c) (f) $\Delta z = 0.7$ mm.

III. Conclusion

Holographic display (HD) provides three-dimensional image with holograms. Light source plays a important role in HD, and require a high degree of coherences for sharp reconstructed images. In this work, we studied the effect of spatial coherence on the image sharpness of a reconstructed hologram. This paper presents a method for implementing holographic projection based on a phase-only CGH. We used an RGG to control the degree of spatial coherence and showed that the degree of spatial coherence changes significantly according to the position of the ground glass plate, i.e., by changing the area of the ground glass plate illuminated by a laser beam. Image sharpness is influenced by the degree of spatial coherence of the light source; image sharpness is proportional to the degree of spatial coherence. By ensuring spatial coherence of a light source, the image quality can be quantitatively optimized with respect to the balance between uniformity and sharpness.

ACKNOWLEDGEMENTS

This research was supported by the Basic Science Research Program through the National Research Founda-

tion of Korea (NRF), funded by the Ministry of Education (2018R1D1A1B07047718) and was partly supported by the 2019 scientific promotion program funded by Jeju National University.

REFERENCES

- [1] T. C. Poon, *Digital holography and three-dimensional display: Principles and Applications* (Springer, New York, 2006).
- [2] M. Kujawinska *et al.*, *Optics Express* **22**, 2324 (2014).
- [3] K. Takano, and K. Sato, *Opt. Eng.* **41**, 2427 (2002).
- [4] K. Hong *et al.*, *Opt. Lett.* **39**, 127 (2014).
- [5] U. Schnars and W. Jueptner, *Digital Holography: Digital Hologram Recording, Numerical Reconstruction, and Related Techniques* (Springer, 2004).
- [6] I. Yamaguchi and T. Zhang, *Opt. Lett.* **22**, 1268 (1997).
- [7] H. Cho, D. Kim, S. Shin, and Y. Yu, *J. Opt. Soc. Korea* **15**, 352 (2011).
- [8] B. Javidi and D. Kim, *Opt. Lett.* **30**, 236 (2005).
- [9] I. Yamaguchi and T. Zhang, *Opt. Lett.* **22**, 1268 (1997).
- [10] M. Tziraki *et al.*, *Appl. Phys. B* **70**, 151 (2000).
- [11] J. Garcia-Sucerquia, J. A. H. Ramírez, and D. V. Prieto, *Optik* **116**, 44 (2005).
- [12] D. Mengu, E. Ulusoy, and H. Urey, *Opt. Express* **24**, 4462 (2016).
- [13] Dorrer, *J. Opt. Soc. Am. B* **21**, 1417 (2004).
- [14] McCutchen, *J. Opt. Soc. Am.* **56**, 727 (1966).
- [15] D. Voelz, *Computational Fourier Optics* (SPIE Bellingham, Washington USA, 2011).
- [16] J.W. Goodman, *Introduction to Fourier Optics, 2nd ed.*, edited by J. Goodman (McGraw Hill, New York, 2005).
- [17] L. E. Estes, L. M. Narducci, and R. A. Tuft, *J. Opt. Soc. Am.* **61**, 1301 (1971).
- [18] T. Stangner *et al.*, *Appl. Opt.* **56**, 5427 (2017).